Insoluble lipid film mediates transfer of soluble saccharides from the sea to the atmosphere: the role of hydrogen bonding

Minglan Xu, Narcisse Tsona Tchinda, Jianlong Li, Lin Du*

Environment Research Institute, Shandong University, Binhai Road 72, Qingdao, 266237, China

Correspondence: Lin Du (lindu@sdu.edu.cn)

Abstract

Saccharides are a large portion of organic matter in sea spray aerosol (SSA). Although they can affect climate-related properties of SSA, the mechanism through which saccharides are transferred from bulk seawater to the ocean surface and ultimately into SSA is still debated. Here, the transfer of small soluble saccharides was validated using a controlled plunging jet sea spray aerosol generator to better understand the wide range of particle properties produced by natural seawater mixed with model organic species, glucose and trehalose. We showed that both soluble saccharides can promote the production of SSA particles, and the presence of trehalose could increase the SSA number concentration by 49.4%. Conversely, the role of the insoluble fatty acid film on the seawater surface greatly reduced the production of SSA. The resulting inorganic-organic mixed particles identified by the transmission electron microscope (TEM) showed typical core-shell morphology. Langmuir model was used to parameterize the adsorption and distribution of saccharide into SSA across the bubble surface, while infrared reflection-absorption spectroscopy (IRRAS) combined with Langmuir isotherms were undertaken to examine the effects of aqueous subphase soluble saccharides with various concentrations on the phase behavior, structure and ordering of insoluble lipid monolayers adsorbed at the air/water interface. We found that the adsorption of glucose and trehalose on the fatty acid monolayer led to the expansion of the mean molecular area. Saccharide-lipid interactions increased with increasing complexity of the saccharide in the order glucose < trehalose. On seawater solution, the effects of dissolved saccharides on the ordering and organization of fatty

acid chains were muted. The enhancement of the carbonyl band to the low wavenumber region implied that soluble saccharides can form new hydrogen bonds with fatty acid molecules by displacing large amounts of water near the polar head groups of fatty acids. Our results indicate that the interaction between soluble saccharides and insoluble fatty acid molecules through hydrogen bonds is an important component of the sea-air transfer mechanism of saccharides.

1 Introduction

Sea spray aerosol (SSA) represents a major source of aerosol particle populations and significantly impacts the earth's radiation budget, cloud formation and microphysics by serving as cloud condensation nuclei (CCN) and ice nuclei (IN), and microbial cycling (Bertram et al., 2018; Partanen et al., 2014). The formation of SSA particles is strongly influenced by the uppermost sea surface microlayer (SML), which is a thin layer of 1–1000 μm thickness formed due to different physicochemical properties of air and seawater (Wurl et al., 2017). Beyond sea salt, the ocean surface contains a fair amount of organic matter (OM) mass fraction, covering carbohydrates, lipids, proteins, humic-like substances (HULIS), intact phytoplankton cells and fragments, fungi, viruses, and bacteria (Van Pinxteren et al., 2020; Cunliffe et al., 2013). These organic matter coincides with some chemical markers that is enriched in the SSA, which is mainly produced by bubble-mediated (Russell et al., 2010; Facchini et al., 2008). When a bubble reaches the water surface, destroying the surface membrane of the water, the bubble bursts into many so-called film drops. After the

bubble film breaks, a jet of water rising vertically from the ruptured bubble cavity forms so-called jet drops. Film drops are responsible for the major proportion (~60%–80%) of submicron particles, whereas jet drops contribute significantly to the production of supermicron particles (Wang et al., 2017). Both the size and chemical composition of SSA are important properties in determining cloud formation and eventually radiative forcing (Brooks and Thornton, 2018). Hence, understanding the physico-chemical mechanisms driving these variations is essential for predicting SSA composition and climate-related processes.

Surface-active biomolecules are preferentially transferred from marine surface water into the atmosphere through the bubble bursting processes, forming a considerable fraction of primary marine organic aerosols (Schmitt-Kopplin et al., 2012). Previous measurements have shown that up to 60% of ocean particle mass can be organic, which exhibits a strong size dependence (O'dowd et al., 2004; Russell et al., 2010). Spectroscopic evidence from field-collected SSA particles indicates that the oxygen-rich organic fractions of individual particles contain molecular signatures of saccharides and carboxylic acids (Hawkins and Russell, 2010). For example, it has previously been observed that the carbohydrate-like spectroscopic signatures account for 40–61% of the submicron SSA organic mass (Quinn et al., 2014; Russell et al., 2010). A large portion of this mass is attributed to saccharides that are transferred from seawater to SSA, and shows a certain enrichment in SSA. Specifically, the high enrichment factor of carbohydrates was calculated for supermicron (20–4000) and submicron (40–167000) particles relative to the bulk seawater in the Western

Antarctic Peninsula (Zeppenfeld et al., 2021). According to previous laboratory studies, marine bacteria, divalent cations and protein can affect the saccharide enrichment in SSA (Hasenecz et al., 2020; Schill et al., 2018). However, a mechanistic and predictable understanding of these complex and interacting processes in favor of saccharides found in marine aerosol particles remains largely unexplored, despite their oceanic and atmospheric significance.

A variety of saccharides have been found ubiquitous in the ocean, including dissolved free monosaccharides, oligo/polysaccharides, sugar alcohols, and monosaccharide dehydrates, the composition of which depends on marine biological activity (Van Pinxteren et al., 2012). Frossard et al. (2014) used the hydroxyl characteristic functional group of atmospheric marine aerosols from Fourier transform infrared spectroscopy to infer the contributions of different saccharides in SSA. It was found that the primary marine aerosols produced in biologically productive seawater had stronger hydroxyl group characteristic of monosaccharides and disaccharides, while the hydroxyl groups of seawater organic matter were closer to those of polysaccharides. This suggests that larger saccharides may be preferentially retained in seawater during aerosol production. Analysis of aerosol samples collected on the Western Antarctic Peninsula also showed that not only polysaccharides but also a high portion of free monosaccharides mainly composed of glucose, fructose, rhamnose and glucosamine were present (Zeppenfeld et al., 2021). Raman spectroscopy was used to measure individual SSA particles generated via wave breaking in a wave flume under algal bloom conditions to get a deeper insight into their organic categories. It was

reported that 4%–17% and 3%–46% of sub- and supermicron particles show strong spectral characteristics of free saccharides and short-chain fatty acids, respectively (Cochran et al., 2017). However, current climate models largely underestimate the ratio of saccharides in marine aerosols (Cravigan et al., 2020), and there is an urgent need to clarify the physicochemical mechanisms that drive saccharides transfer to SSA.

A possible explanation for the origin of saccharides in SSA chemical composition involves the affinity between the bulk aqueous soluble saccharides and insoluble surfactant monolayers already adsorbed at the air/water interface, resulting in co-adsorption of the soluble saccharides (Link et al., 2019b). This co-adsorption arises from non-covalent interactions and promotes the binding of soluble organic matter to the surface with insoluble Langmuir film. Previous studies have indicated that the presence of lipids or proteins strongly enhances the surface adsorption capacity of saccharides, even for highly soluble saccharides that do not adsorb individually at the air/water interface (Pavinatto et al., 2007; Burrows et al., 2016). For example, recent studies have shown that simple, soluble biomolecules such as phenylalanine and trehalose exhibit an affinity for lipid films, altering membrane permeability and phase behavior (Perkins and Vaida, 2017; Link et al., 2019a). A divalent cation-mediated co-adsorption mechanism was also proposed to explain the enrichment of monosaccharide in laboratory-generated SSA (Schill et al., 2018). Alternatively, saccharides can be bound covalently to larger, more surface-active biomolecules, such as glycoproteins or lipopolysaccharides, which attach to SML and are eventually

117 transferred into SSA through bubble bursting at the ocean surface (Estillore et al.,
118 2017). Although different hypotheses have been proposed, there is still debate about
119 the more nuanced mechanisms that guide the sugar-lipid interactions in the marine
120 environment.

121 The present work aims to use a multipronged approach that combines bulk SSA
122 production experiments, Langmuir surface pressure-area isotherms and infrared
123 reflection-absorption spectroscopy (IRRAS) to examine the role of saccharides in
124 SSA production and the mechanism of saccharides transfer and enrichment from
125 aqueous solution into SSA. The study focuses on two soluble saccharides that are
126 prevalent in seawater, glucose and trehalose, which are uncharged monosaccharide
127 and disaccharide, respectively. A plunging jet sea spray aerosol generator was used to
128 generate nascent SSA particles by artificially generating bubbles in seawater as a
129 mean of simulating sea spray production by breaking waves. This simulation helps
130 evaluate the impact of soluble saccharides as well as insoluble fatty acids on SSA
131 production and particle morphology. Langmuir isotherms provided abundant
132 information for stability and fluidity of monolayers, which were used to adequately
133 describe the magnitude of interaction effects between subphase soluble saccharides
134 and surface insoluble surfactants. Finally, IRRAS spectra provided molecular scale
135 descriptions of monolayer conformational information and allowed us to deduce the
136 distribution of saccharide species at the interface. By combining all the findings, we
137 propose a model of sea-air transfer of marine saccharides through hydrogen bond
138 interactions involved in surface insoluble lipid molecules.

2 Experimental sections

2.1 Materials and solutions

D-(+)-Glucose (Glu, powder, ≥99.5%) and D-(+)-Trehalose anhydrous (Tre, powder, 99%) were purchased from Aladdin. Stearic acid (SA, >98%, TCI), palmitic acid (PA, >98%, Adamas-beta) and myristic acid (MA, ≥99.5%, Aladdin) were prepared in chloroform (AR, ≥99.0%, Sinopharm Chemical Reagent Co., Ltd) at a final concentration of 1 mM each. Fig. S1 shows the chemical structures of the three fatty acids used in this study. The respective fatty acid solutions were mixed at a molar ratio of 2 MA:4 PA:3 SA to obtain a mixed lipid stock solution considering that PA and SA account for approximately two-thirds of the total saturated fatty acids in fine SSA particles, with MA being the third most abundant species (Cochran et al., 2016). All chemicals were used without further purification. The natural seawater (SW) was collected from Shazikou, Qingdao, China. Here, surface seawater (within 0.1~1 m below the sea surface) was obtained from a pier on the coast by immersing high-density polyethylene containers into the water. The sampled seawater was microfiltered through 0.2 μm polyethersulfone filter (Supor®-200, Pall Life Sciences, USA) to remove large particles such as sediments, algae and bacteria. The filtered seawater was used for SSA generation and as a filling subphase for interfacial experiments. The pH of natural seawater, initially determined to be about 8.13±0.02, was measured to be around 8.04±0.01 at the end of the experiment. Different concentrations of saccharide-containing seawater solutions required in the

experiments were obtained by dissolving different masses of glucose or trehalose in the filtered natural seawater using mechanical stirring.

2.2 SSA production and collection

SSAs were produced using a plunging jet-sea spray aerosol generator (Fig. 1). A physical drawing of the aerosol generation system can be found in Fig. S2. The generator and its detailed operation principle has been described elsewhere (Liu et al., 2022). Briefly, the generator consists of a stainless steel (shipboard class, 316L) rectangular sealed container and a viewable glass window. The upper removable lid has ports for water inlet, purging air, and sampling. The purge air is supplied by a zero-air generator (Model 111, Thermo Scientific, USA) and the flow rate is controlled at 10 L min^{-1}. A peristaltic pump (WL600-1A, ShenChen) periodically circulates water from the bottom of the generator to the top nozzle through a Teflon tube with a pump speed of 1 L min^{-1}, creating a plunging water column that hits the seawater surface and entrains air into the bulk seawater. The bubble plumes extend approximately 15 cm down into the water, a moderate depth considering that the majority of the air being entrained in is located within about 50 cm from the sea surface (Hultin et al., 2010). When the bubbles rise to the air/water interface and burst, they generate SSA emissions. When studying insoluble surfactant effects, a concentrated solution of 1 mM mixed fatty acids in chloroform was added to the surface of the seawater solution. After the necessary fatty acids were added, only the sheath air flowed, allowing the chloroform to evaporate for 15 min and leaving only

the surfactant on the surface. After pre-preparation for 15 min, the sheath air and peristaltic pump were turned on to produce SSAs. Prior to collection, SSAs were dried to a relative humidity of ~40% using a diffusion dryer. Thereafter, a scanning mobility particle sizer (SMPS, model 3936, TSI) consisting of a differential mobility analyzer (DMA, model 3081, TSI Inc., USA) and a condensation particle counter (CPC, model 3776, TSI Inc., USA) was used to measure the particle size distributions and number concentrations. The particle size distribution ranging from 13.6 to 710.5 nm was obtained at a sheath flow rate of 3.0 L min^{-1} and aerosol flow rate of 0.3 L min^{-1}. Dried SSAs were deposited onto 200 mesh copper grids with carbon foil (T11023, Tilan, China) by a single particle sampler (DKL-2, Genstar electronic technology Co., Ltd) to further characterize the particle morphology.

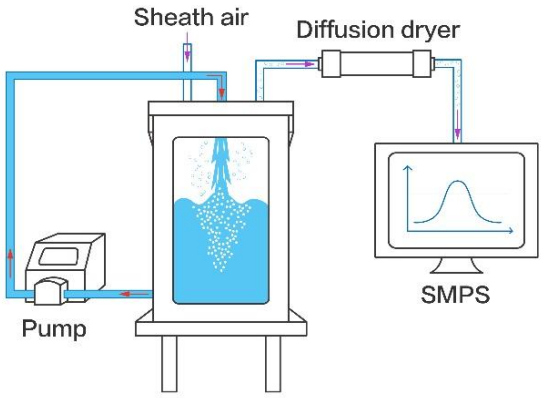

Figure 1. Schematic picture of the plunging jet-sea spray aerosol generator. The red arrows represent the flow direction of seawater, and the purple arrows represent the flow of gases and aerosols.

2.3 Langmuir monolayer preparation and Langmuir isotherms

The Langmuir trough setup has been described previously (Xu et al., 2021). Briefly, it consists of a rectangular Teflon trough (Riegler & Kirstein, Germany) and two moveable Teflon barriers whose movements are precisely controlled to achieve symmetric compression of the monolayer at the air/water interface. A Wilhelmy plate attached to the pressure sensor was used to measure the surface pressure. Each 100 mL subphase consisted of natural seawater, with varying amounts of glucose or trehalose. Aliquots of mixed fatty acids stock solution were spread onto the subphase surface dropwise with a glass microsyringe and 15–20 min were allowed for solvent evaporate completely. The surface pressure (π), given by eq 1 and defined as the difference in surface tension between the pure air/water interface (γ_0) and the monolayer covered interface (γ) was monitored.

$$\pi=\gamma_0-\gamma \quad (1)$$

The barriers were compressed at a rate of 3 mm min^{-1} per barrier and isotherm data were collected for surface pressure π (mN m^{-1}) versus area per molecule ($Å^2$). All experiments were performed at (22 ± 3) ℃ and relative humidity below 65%.

2.4 Infrared reflection-absorption spectroscopy measurement

The polarization-modulation infrared reflection-absorption spectroscopy (PM-IRRAS) is a mainstream spectroscopic method for in-situ characterization of Langmuir monolayers at the molecular level. For IRRAS spectra, floating monolayers were spread at the aqueous subphase and compressed to the desired surface pressure, and

stopped before obtaining the spectra. PM-IRRAS spectra were obtained using a Fourier transform infrared (FT-IR) spectrometer (Bruker Vertex 70, Germany) equipped with an external reflection accessory (XA-511). The interference infrared beam was set out from FT-IR and polarized by a ZnSe polarizer to alternately generate s- and p-polarization lights. They were then continuously modulated by a photoelastic modulator (PEM-100) at a high frequency of 42 kHz to measure the spectra of both polarizations simultaneously. The infrared beam was focused onto the Langmuir film through a gold mirror, and then a portion of reflected light was directed onto the liquid nitrogen-cooled mercury-cadmium-telluride (MCT) detector. The application of polarization modulation attenuates the noise of reflective FT-IR and the interference of water vapor and carbon dioxide. The spectra presented here are reflectance-absorbance (*RA*) given as:

$$RA = -\log(R/R_0) \quad (2)$$

where R and R_0 are the reflectance of fatty acid monolayer and pure seawater solution surface, respectively. To obtain a better signal-to-noise ratio, spectra were collected with 2000 scans and 8 cm^{-1} resolution at a fixed incidence angle of 40°. To better compare the variation in the spectral region of interest, peaks were fitted to Gaussian functions using Origin 2021 for each displayed spectrum.

2.5 Transmission electron microscope imaging

Particle imaging was performed using a transmission electron microscope (TEM, FEI Tecnai G2 F20, FEI, USA) equipped with a Schottky field emission gun. It was

operated at an accelerated voltage of 20–200 kV with a high angle annular dark field detector to collect TEM images and even preserve the soft internal structure of organic sources under high vacuum conditions.

3 Results and discussion

3.1 SSA particle number size distributions

To examine the sea-air transfer of soluble saccharides and their interaction with insoluble fatty acids, SSA particle generation experiments were carried out with seawater containing 1.0 g L^{-1} glucose or trehalose. Figure 2 shows the particle number size distributions resulting from seawater to which different soluble saccharides were added in the presence or absence of fatty acids on the surface. As a reference, the particle size distribution produced from natural seawater is also given. The submicron particle size distributions produced by the plunging jet generator are well represented by lognormal mode. In the absence of saccharide, a broad, unimodal mode of the particle size distribution around 168 nm was generated. This observation agrees quite well with a previous study that produced SSA by the plunging jet method with the mode of the particle size distribution ~162 nm (Christiansen et al., 2019). Moreover, the SSA yielded by plunging waterfall also has a size distribution similar to that yielded by the breaking wave, which particle number size distribution is ~162 nm (Prather et al., 2013). This contrasts with most previous laboratory studies using sintered glass filters or frits, which tend to exhibit a smaller mean diameter and narrower distribution. This may be expected, given that similar bubble size

distributions exist in the two generation mechanisms using plunging waterfall and breaking waves. A previous study using plunging jets has produced similar bubble size distributions (Fuentes et al., 2010). Importantly, the measured bubble spectrum for the breaking waves matches the shape and Hinze scale of the bubble spectra of the previously measured open ocean breaking waves (Deane and Stokes, 2002). Although we did not directly measure the bubble spectra generated by the plunging jet method in this study, it should be able to better simulate the properties of breaking waves according to the above empirical studies. Moreover, we compared the particle size distributions of SSA generated in our laboratory with those measured in field studies (Quinn et al., 2017; Xu et al., 2022). As shown in Fig. S3, it was observed that the size distribution of both laboratory-generated SSAs and SSAs measured in the field had a major accumulation mode in the range of ~111–172 nm. However, the number concentration of SSAs produced in our experiment is about 2 orders of magnitude higher than that in the real environment. As a result, the jet sea spray generator system is capable of a wide range of measurements (e.g., size-resolved hygroscopicity and heterogeneous reactivity) that are not achievable at low number concentrations.

Laboratory studies of the effects of saccharide organic substances on droplet production have been inconclusive. A previous study has used two bubble generation methods (plunging water jet and diffusion aeration) to investigate the number size distribution of SSA particles produced by mixing fructose and mannose with NaCl or artificial seawater solution (King et al., 2012). The results showed that the number concentration of particles produced by artificial seawater containing sodium dodecyl

sulfate was significantly lower than that of particles produced by artificial seawater containing fructose. However, NaCl solution containing mannose produced SSA with lower number concentration than NaCl solution containing sodium laurate. Lv et al. (2020) found that addition fructose to sea salt solution can significantly promote the increase of SSA number concentration. However, the above studies lacked direct comparative results on SSA production influenced by different soluble saccharides. For the plunging jet, our measurements indicate that soluble saccharides can promote the production of SSA to varying degrees. The number concentration, mass concentration, and geometric mean diameter are shown in supplement Table S1 for further details. It was observed that glucose led to a slight increase of about 15.6% in particle number concentration, increasing the mode diameters to ~175 nm. In contrast, the natural seawater spiked with trehalose resulted in a higher total particle number concentration that increased by approximately 49.4% over a wide size range. Therefore, the changes in production and properties of SSA from actual seawater may be more complicated under the influence of different saccharides.

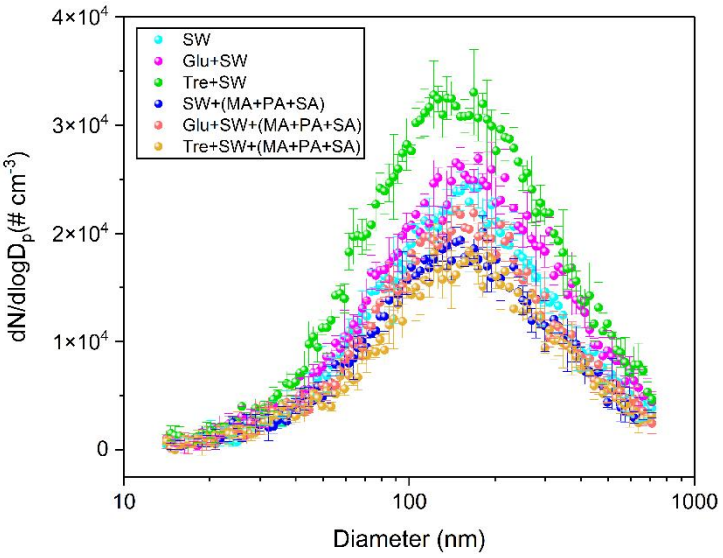

296

297 **Figure 2.** The particle number size distribution spectra of SSAs produced from blank
298 seawater sample and seawater sample spiked with glucose or trehalose. Both results
299 are presented here with and without fatty acid surface films.

300 The effect of the interaction of insoluble fatty acids with different saccharides on
301 SSA particles was investigated by spreading insoluble fatty acids on seawater surface.
302 In plain sight, fatty acids on the surface can significantly reduce the number
303 concentration of SSA regardless of the presence of saccharides in the seawater. When
304 the fatty acid surfactant was added to seawater alone, the number concentration
305 decreased by about 17.2%, while the presence of glucose resulted in a decrease of
306 about 21.6%. Moreover, fatty acids showed the highest inhibitory effect on SSA
307 produced by trehalose-containing seawater solution, whose concentration decreased
308 by about 49.4%. We ascribe that the surface layer is significantly more stable in the
309 presence of fatty acids, even when disturbed by the plunging jet, thus resulting in less
310 bubble bursting. Furthermore, the continuous plunging caused a layer of foam to
311 accumulate on the surface of the water. The presence of the foam layer on the

seawater surface may be capable of prohibiting the production of droplets by assimilating rising bubbles into the foam layer before bursting. Collectively, the observed variability in these experiments suggests an urgent need to better build the link between total SSA particle flux and seawater organic composition over the ocean. However, sole bulk-phase generation experiments may not accurately capture the relevant chemical behaviors and support mechanism analysis that occur in the SML. Therefore, we attempted to explore the possible interaction mechanisms via air/water interface chemical experiments.

3.2 π-A isotherms of fatty acid monolayers

In this section, we only discuss traditional Langmuir monolayers, which operate on air/water interfaces that are ubiquitous along the sea surface (Elliott et al., 2014). The π-A isotherm reflects information on the phase behavior of the monolayer as a function of lipid packing density. As shown in Fig. 3, the π-A isotherms of individual and mixed fatty acids on the natural seawater subphase are presented. When the mechanical barriers initially begin to compress, the amphiphilic molecules in the monolayer are in the gaseous (G) phase under a large area per molecule, with the hydrophobic tails having significant contact with the water surface, but little contact with each other. At this stage, the compression of the film does not lead to a significant change in surface pressure. As the monolayer is compressed, the intermolecular distances gradually decrease and the surface pressure begins to rise from zero into the liquid expanded (LE) phase, where the hydrophobic tails start to

touch each other, but remain largely disordered and fluid. This is represented as the lift-off area of the isotherm. Further compression results in a thermodynamic transition to a liquid condensed (LC) phase. The film is eventually compressed to a limiting point where the monolayer collapses as the materials leave the 2D film (Lee, 2008). In general, the collapse is an irreversible process, and the collapsed material does not reintegrate into the monolayer as the surface pressure decreases.

Although the π-A isotherms of individual fatty acids have been well studied, the phase behavior of the mixed binary and ternary systems still needs to be further explored. Pure natural seawater without spreading surface-active fatty acids does not cause observable changes in the surface pressure, indicating that surface-active impurities are either absent or have too low concentrations to cause film formation. When myristic acid spreads on the water surface, it undergoes a long liquid phase, with a lower collapse pressure of ~27 mN m^{-1} and area per molecule as low as 5 $Å^2$. This is due to the relatively high solubility of MA molecules in the aqueous phase, resulting in a large loss of molecules in the monolayer under the mechanical forcing from lateral barriers compression. In addition, according to the surface pKa value of 7.88 at 20 °C, MA is mostly deprotonated at pH ~8.1, so a stable monolayer cannot be obtained for the natural seawater subphase due to the dissolution phenomenon (Carter-Fenk and Allen, 2018). For palmitic acid monolayer, it goes through a relatively short gaseous phase and rapidly enters the liquid phase. After experiencing a kink point at ~48 mN m^{-1}, it continues to rise to the maximum surface pressure of ~57 mN m^{-1} and collapses. Both the lift-off area and molecular area of the stearic acid

355 film decreased more than those of palmitic acid film. This is caused by the fact that
356 the interaction (van der Waals force) between the molecules increases as the
357 molecular weight of long chain fatty acid increases. That is, increased attraction leads
358 to a decrease in distance between SA molecules.

359 When fatty acids are mixed in a certain molar ratio and spread onto the interface
360 water, it is found that the π-A isotherm lies between the pure fatty acids and is closer
361 to that of stearic acid, but the mean molecular area is relatively smaller. The partial
362 dissolution of myristic acid most likely accounts for the smaller mean molecular area
363 observed in the proxy mixture isotherm compared to the palmitic acid and stearic acid
364 isotherms. Moreover, we found that the π-A isotherms of mixed fatty acids exhibit
365 similar collapsing behavior to those of stearic acid and palmitic acid at a surface
366 pressure of about 50 mN m^{-1}. Consequently, the longer fatty acids will dominate the
367 lateral interactions of the SSA membrane, which makes the membrane more rigid due
368 to the larger sum of diffusive interactions. In view of the true proportion of fatty acids
369 in the nascent sea spray particles, we used a ternary fatty acid membrane proxy
370 system composed of MA, PA, and SA (2:4:3 molar ratio) in the following experiments
371 involving Langmuir isotherms.

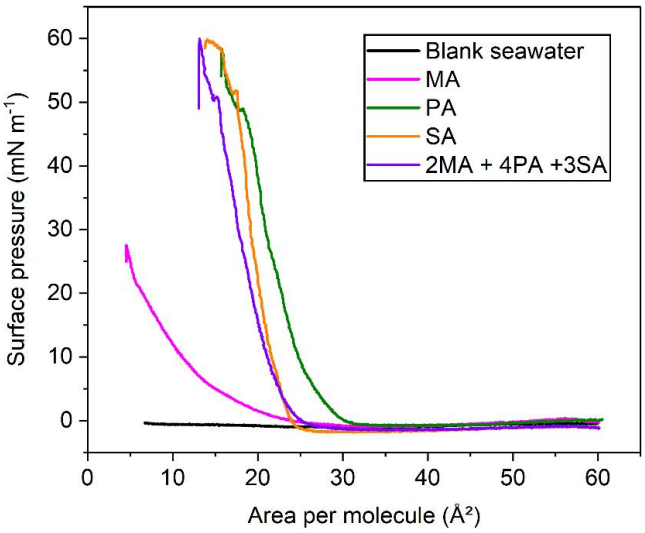

Figure 3. π-A isotherms of myristic acid, palmitic acid, stearic acid and mixed fatty acids. The black trace represents the background natural seawater solution with no fatty acid spread.

3.3 Effect of soluble saccharides on the phase behavior of mixed monolayers

An effective way to test whether soluble saccharides associate with lipid membranes is to examine the effect of these saccharides on the phase behavior of lipid films. The π- A isotherms provide insights into the overall monolayer structure, intermolecular interactions, and the adsorption of glucose and trehalose. Both glucose and trehalose are highly soluble (>1.0 g L^{-1}) in water. However, this solubility does not preclude their presence on the surface. According to some previous studies, the dissolved organic carbon concentration is about 0.7–1.0 mg carbon L^{-1} (Quinn et al., 2015; Hasenecz et al., 2019). Considering that saccharides in the ocean represent approximately 20% of the dissolved organic carbon (Pakulski and Benner, 1992; Hasenecz et al., 2019), the saccharide concentration is about 0.14–0.20 mg L^{-1}. The glucose and trehalose concentrations used for the π-A isotherms are approximately

388 3–4 orders of magnitude greater than the saccharide concentration in dissolved
389 organic matter, maintaining detectivity within the π-A isotherms. Furthermore, high
390 concentrations used here are still relevant, considering the evaporation process in aged
391 sea spray aerosols (Hasenecz et al., 2020). At the same time, such concentrations are
392 close enough to understand the enrichment of saccharides in sea surface microlayer
393 and to provide a confident interpretation of the physicochemical mechanisms driving
394 the adsorption and transfer of soluble saccharides (De Vasquez et al., 2022).

395 Figure 4 shows the π-A isotherms of mixed fatty acids on natural seawater
396 subphases containing different concentrations (varied between 0.1 and 5.0 g L^{-1}) of
397 glucose or trehalose. In this case, the surface pressure and mean molecular area of the
398 fatty acid monolayer is equal to that of the fatty acid monolayer with the addition of
399 saccharides, provided that the saccharide molecules do not affect the monolayer. At a
400 low concentration of 0.1 g L^{-1}, both saccharides had little overall effect on the phase
401 behavior of fatty acid monolayers. However, they resulted in a smaller lift-off area for
402 the monolayer compared to pure natural seawater. As the glucose and trehalose
403 subphase concentration increases, the monolayers are expanded, taking up a larger
404 mean molecular area, which is consistent with previous research (Crowe et al., 1984).
405 This noticeable expansion can be observed from the lift-off area to collapse,
406 indicating that saccharides participate in and disrupt the monolayer structure, and
407 implying a degree of complexity and heterogeneous distribution of species in the
408 interfacial region. De Vasquez et al. (2022) also demonstrated that glucuronate
409 interacts with and expands the stearic acid monolayer. Furthermore, they suggested

that glucuronate intercalates into the stearic acid monolayer and leads to monolayer reorganization. Spectral evidence is needed to further clarify whether intercalation occurs in our study.

More surprisingly, we observed that the isotherms of the two saccharide matrices do not exhibit much difference at the concentrations of 0.5 g L^{-1} and 1.0 g L^{-1}. When the saccharide concentration keeps increasing to 5.0 g L^{-1}, the molecular packing density on the interface decreases, and the apparent molecular area increases. In the presence of glucose and trehalose, the lift-off areas increased by 9 and 10 $Å^2$, respectively. Another distinguishing feature of the fatty acid isotherms is the change of slope above ~40 mN m^{-1}. This result could be interpreted as the saccharide being "squeezed" out of the insoluble film, resulting in higher monolayer compressibility. By squeezing saccharide molecules out of the monolayer, the isotherms at high surface pressure behave similarly to other isotherms with low saccharide concentrations. The difference is that with the increase of structural complexity of saccharide, the effect of trehalose at the same concentration is more prominent. The α, α, 1,1-linkage between two glucose subunits in trehalose is considered to provide an elastic and rigid balance, thus allowing for strong interactions with multiple fatty acids (Clark et al., 2015). As a result, trehalose binds more readily to lipid monolayer surfaces than glucose, as is evident from experimental observations. This is consistent with the result of Crowe et al. on the effect of saccharides (glucose and trehalose) on the properties of 1,2-dimyristoyl-*sn*-glycero-3-phosphocholine (DMPC) and 1,2-dipalmitoyl-*sn*-glycero-3-phosphocholine (DPPC) monolayers. That is, the area

per lipid increases with the increase of saccharide concentration, and trehalose provides the largest lateral monolayer expansion (Crowe et al., 1984). The expansion effect promoted by soluble saccharides is more relevant at lower surface pressure when alkyl chains are farther apart from each other. Clarifying and refining the interaction mechanisms by which lipid molecules interact with saccharides is critical to any attempt to model such chemical phenomena occurring at environmentally relevant interfaces.

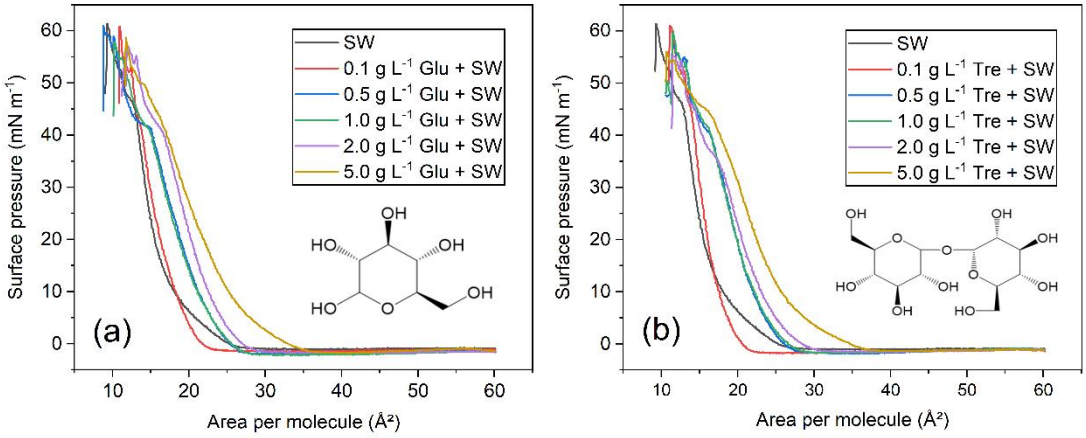

Figure 4. π-A isotherms of mixed fatty acids in the SW subphase with several concentration gradients of (a) glucose, and (b) trehalose. The inset shows the molecular structures of glucose and trehalose.

3.4 Effect of soluble saccharides on the interfacial structure of mixed monolayers

PM-IRRAS is a surface sensitive technique that allows further study of the possible effects of soluble saccharides on lipid interfacial organization at the molecular level. Figure 5 shows the IRRAS spectra for mixed fatty acid monolayers at two different saccharides containing subphases at a surface pressure of ~30 mN m^{-1} to ensure complete monolayer formation. Figure S4 shows the IRRAS spectra of mixed fatty

449 acids measured at different surface pressures. It can be observed that with the increase
450 of surface pressure, the intensity of the peaks also increases accordingly, reaching a
451 relatively stable level around 30 mN m^{-1}. Considering the stability of the monolayer,
452 this surface pressure was chosen to obtain the desired infrared spectra.

453 The absorption band in the 3000–2800 cm^{-1} region shown in Fig. 5 is ascribed to
454 the CH stretching vibration of the alkyl chain. The main features at ~2916 and ~2850
455 cm^{-1} are related to antisymmetric ($\nu_{as}(CH_2)$) and symmetric ($\nu_s(CH_2)$) stretching
456 modes of methylene of mixed fatty acids, respectively. The $\nu_{as}(CH_2)$ feature
457 consistently remains stronger than $\nu_s(CH_2)$ with the increase of glucose and trehalose
458 concentrations. These two band positions are often used to be empirically correlated
459 with the order and organization within the alkyl monolayer adsorbed to the water
460 interface, with higher wavenumbers corresponding to disordered *gauche* conformers.
461 Conversely, low wavenumbers indicate that the alkyl chain of lipids is well ordered
462 with preferential *all-trans* characteristics. Additionally, we also showed the
463 wavenumbers, reflectance-absorbance intensities, peak areas and full width at half
464 maximum (FWHM, cm^{-1}) values of each fitted peak in Table S2 in the supplement. In
465 this work, the relatively low frequencies of $\nu_{as}(CH_2)$ (2916–2918 cm^{-1}) and $\nu_s(CH_2)$
466 (2848–2851 cm^{-1}) hint that the molecular conformation of the fatty acid alkyl chains
467 is dominated by the highly ordered *all-trans* conformation (Li et al., 2019). Despite
468 the concentration range of saccharides varied widely, the positions of $\nu_{as}(CH_2)$ and
469 $\nu_s(CH_2)$ showed modest sensitivity to shift, suggesting very minor changes in the
470 conformation of the alkyl chain. The relative weak antisymmetric ($\nu_{as}(CH_3)$) and

symmetric methyl stretching ($\nu_s(CH_3)$) vibrations were observed at ~2958 and ~2880 cm^{-1}, respectively. These results indicate that the penetration of soluble saccharides is only superficial (along the lipid surface) and has little effect on the alkyl tail arrangement. Therefore, it is further deduced that the stabilization mechanism between saccharides and fatty acid molecules may occur in the headgroup region.

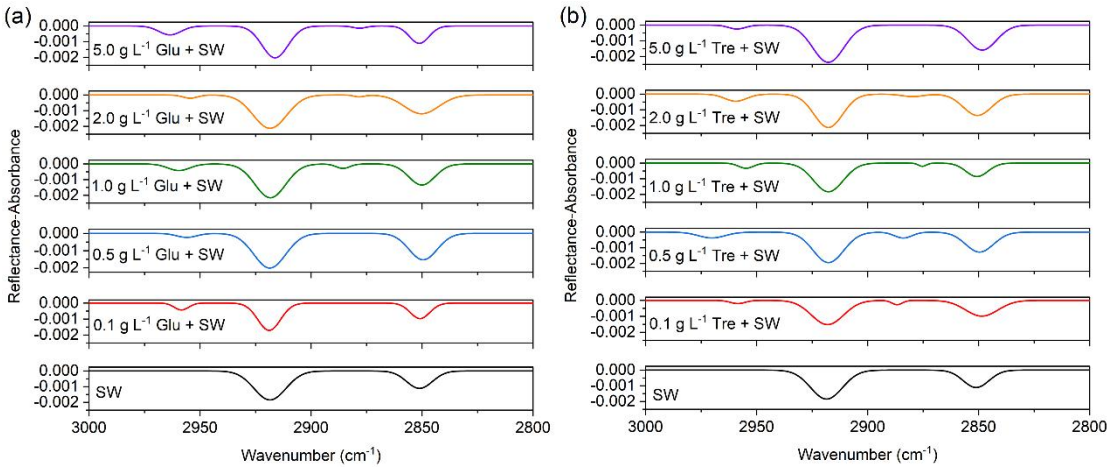

Figure 5. PM-IRRAS spectra (3000–2800 cm^{-1}) of mixed fatty acids at the air/seawater interface at different (a) glucose, and (b) trehalose concentrations in the subphase.

Carboxylic acids possess one hydrogen bond donor (hydroxyl) and one hydrogen bond acceptor (carbonyl) within the same functional group, the carboxyl group. The carbonyl stretching modes (ν(C=O)) of the carboxyl group at ~1734 cm^{-1} (unhydrogen bonded), 1725 cm^{-1} (singly hydrogen bonded) and 1708 cm^{-1} (doubly hydrogen bonded) were observed in seawater (Gericke and Huhnerfuss, 1993), with the strength at 1734 cm^{-1} being the highest (Fig. 6). This band component at 1734 cm^{-1} is put down to the conformation with the carbonyl group almost parallel to the water surface and the hydroxyl group is oriented toward the water surface, which is not conducive

488 to the formation of hydrogen bond with water subphase (Muro et al., 2010). For
489 saccharide concentrations ranging from 0.1 to 2 g L^{-1}, the unhydrated C=O band was
490 observed to be depressed, and the singly and doubly hydrogen bonded carbonyl
491 components at ~1720 and ~1708 cm^{-1} became dominant (Johann et al., 2001). At the
492 highest glucose concentration, the Langmuir model appears to capture a saturation
493 effect, where the establishment of hydrogen bonds is associated with a strong initial
494 increase in glucose organic enrichment, followed by surface saturation at higher
495 organic concentration. We also displayed the wavenumbers, reflectance-absorbance
496 intensities, peak areas and full width at half maximum (FWHM, cm^{-1}) values of each
497 fitted peak in the region of 1800–1300 cm^{-1} in Table S3 in the supplement. The
498 presence of hydrogen bonds between saccharides and the carbonyls of fatty acids is
499 well correlated with the observed shifts in the infrared absorption band of carbonyl
500 groups. Using FTIR experiments, Luzardo et al. (2000) showed that trehalose shifts
501 the vibrational frequency of the carbonyl group to a lower value, which is an evidence
502 of the existence of direct hydrogen bonding between trehalose and lipid carbonyl
503 groups. We believe that saccharides displace water surrounding the fatty acid polar
504 headgroups and interact strongly with lipid headgroups, resulting in a slight decrease
505 in hydration near the monolayer interface.

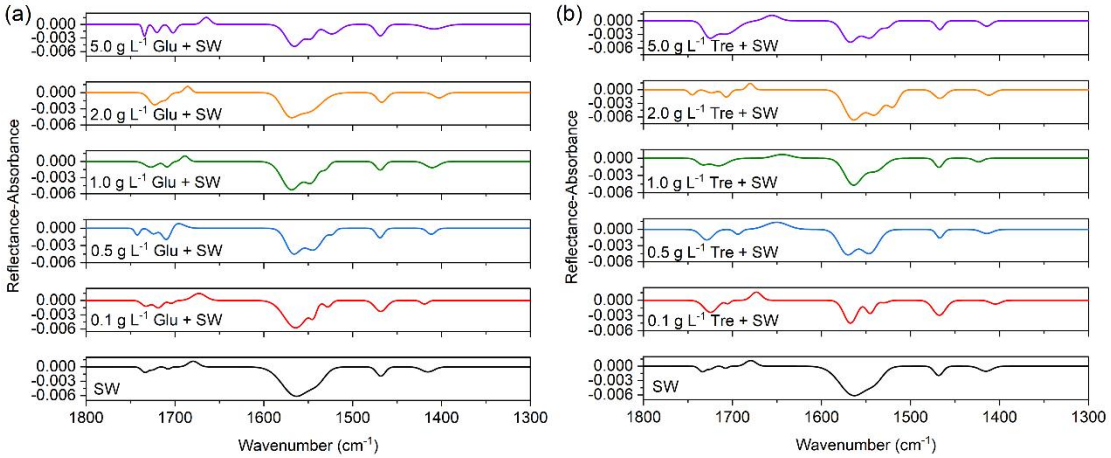

506

507 **Figure 6.** PM-IRRAS spectra (1800–1300 cm^{-1}) of mixed fatty acids at the
508 air/seawater interface at different (a) glucose, and (b) trehalose concentrations in the
509 subphase.

510 The nonmonotonic hydrogen bond strength shows that the interaction at the
511 interface manifests as competing contributions that dominate at different
512 concentrations. Within the concentration range studied, saccharides tend to “displace”
513 water, creating unique environments. In some recent studies, this “water displacement”
514 hypothesis was supported by molecular dynamics (MD) simulations, fluorescence
515 microscopy and nuclear magnetic resonance (NMR) (Lambruschini et al., 2000; You
516 et al., 2021; Kapla et al., 2015). Previous MD simulation studies showed that the
517 hydrogen bond lifetime between trehalose and membrane was longer than that
518 established between water and membrane (Villarreal et al., 2004). This is because
519 water molecules are more mobile and can exchange more frequently at the interface
520 than trehalose. Another study also confirmed that sugar-lipid hydrogen bonds are
521 stronger than water-lipid hydrogen bonds due to low endothermicity and they remain
522 largely intact even at very high sugar concentrations (You et al., 2021). During SSA
523 production, the bubbles remain on the surface for a period of time during which the

bubble's film cap is expelled (Modini et al., 2013), and water and soluble molecules are removed from the bubble film, a process that is thought to be important for the high organic matter fraction. These experiments suggest that there are strong hydrogen bonds between saccharides and fatty acid molecules, so that saccharide molecules may still be bound to the fatty acid monolayer and not be washed out as the film cap drains.

Long chain fatty acid amphiphiles that spread as a monolayer on the alkaline subphase undergo dissociation. The ratio of neutral fatty acids and ionized carboxylates in the monolayer depends on the pH of the subphase solution. At natural oceanic conditions (pH~8.1), deprotonation of the carboxylic acid groups results in two carboxylate stretches. The broad and strong antisymmetric carboxylate stretch (ν_{as}(COO)) were observed at ~1564 cm^{-1}, and the symmetric carboxylate stretch (ν_{s}(COO)) at ~1415 cm^{-1}. The presence of salt in seawater caused the ν_{as}(COO) to split into three peaks at ~1564, ~1544 and ~1528 cm^{-1}. Additionally, we found a shift in the major carboxylate stretching mode from 1564 to higher frequency ~1572 cm^{-1}, which may be indicative of carboxylate dehydration upon interactions with saccharides. Another distinctive feature in all spectra obtained at ~1469 cm^{-1} was assigned to the CH_2 scissoring vibration ($\delta(CH_2)$) of the aliphatic chain (Muro et al., 2010). This wavenumber value somewhat indicates an orthorhombic subcell structure. It should be noted that the $\delta(CH_2)$ vibrational position for the surface membrane of the mixed fatty acids reported here is relatively insensitive to saccharides and their concentrations. This observation confirms the conclusions drawn from the $\nu_{as}(CH_2)$

and $\nu_s(CH_2)$ wavenumbers that higher alkyl chain conformational orders are obtained either on the surface of pure seawater or on subphases containing glucose or trehalose.

3.5 Effect of soluble saccharides on particle morphology

Particle morphology can affect the surface composition, heterogeneous chemistry, gas-particle partitioning of semi-volatile organics and water uptake of aerosols (Unger et al., 2020; Ruehl et al., 2016; Lee et al., 2021). We examined the particle morphology and qualitatively compared SSAs between different model systems, including the mixed effects of saccharides and fatty acids. Compared to the study by Unger et al. (2020), the samples we investigated had compositions that were closely connected to the chemical composition of sea spray aerosols.

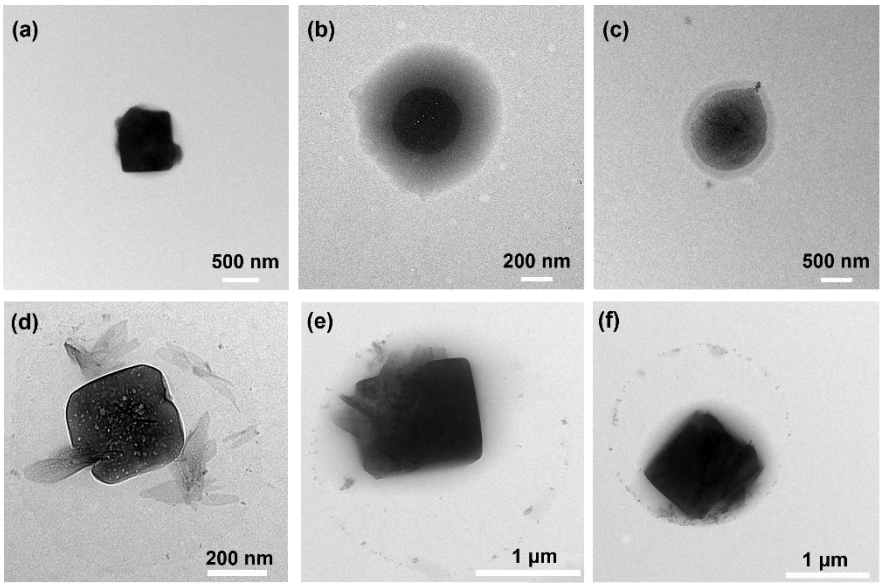

Figure 7. TEM images of morphology identified for sea spray aerosols produced from (a) natural seawater, (b) seawater with glucose and (c) seawater with trehalose without fatty acids organic layer; (d) natural seawater with fatty acids, (e) seawater with glucose and fatty acids, (f) seawater with trehalose and fatty acids.

Figure 7 depicts TEM images of SSA particles generated by plunging jet sea spray aerosol generator, which can provide clues about how saccharide and/or fatty acid components are interacting with sea salt. As can be seen from the Fig. 7a, SSA produced from pure natural seawater by plunging jet exhibited a prism-like morphology that is predominantly inorganic in nature (Lee et al., 2020). This standard cubic shape also suggests that NaCl is an important component of natural seawater sample used in this study. The morphology of SSA particles was strongly affected by the incorporation of saccharides. In the presence of saccharides, the images indicate that these SSA particles exhibit a core-shell morphology with the shell portion being mainly organic in composition, whereas sea salt core are more spherical in nature, demonstrating that organic substances inhibit the cubic crystallization of NaCl. The core-shell morphologies adopted here are congruent with previous studies on the NaCl/Glucose binary system and authentic SSA samples observed using atomic force microscopy (Ray et al., 2019; Estillore et al., 2017). However, as shown in Figs. 7d–f, the presence of fatty acid layer on the surface not only reduces the number concentration of SSA produced but also tends to maintain the cubic shape of the core of SSA. When fatty acids and saccharides coexist, we can still observe the preservation of core-shell structure. In a word, the results presented in this study suggest that the heterogeneity within a particle type is a function of seawater chemistry.

3.6 Proposed mechanism for bulk saccharide transfer to SSA

The molecular level interactions between small saccharides and fatty acids discussed in previous sections can be summarized using the model presented in Fig. 8. Aqueous aerosols coated by surface-active organic matter (Fig. 8a), such as SSA, generally hold inverse micelle structures with hydrophilic headgroups pointing toward the aqueous phase and hydrophobic tails pointing toward the gas phase (Blackshaw et al., 2019). At the center of the inverse micelle, a water pool is formed that can dissolve polar substances such as saccharides, proteins, enzymes, amino acids and nucleic acid. This unique physicochemical environment may enhance the possibility of saccharides transfer to SSA. Through the Langmuir surface pressure-area experiment combined with infrared reflection-absorption spectroscopy, we initially explored the possible mechanism of the transfer of saccharides at the air/water interface. In a nutshell, we infer that saccharides initially in the aqueous phase move steadily to the interface and act as a substituent for water molecules, and locate in the headgroup region of the fatty acids. During the binding process, the saccharides displace the oriented water molecules that are bound to the fatty acids through hydrogen bonds, establishing new hydrogen bonds with the carbonyl group of fatty acids (You et al., 2021).

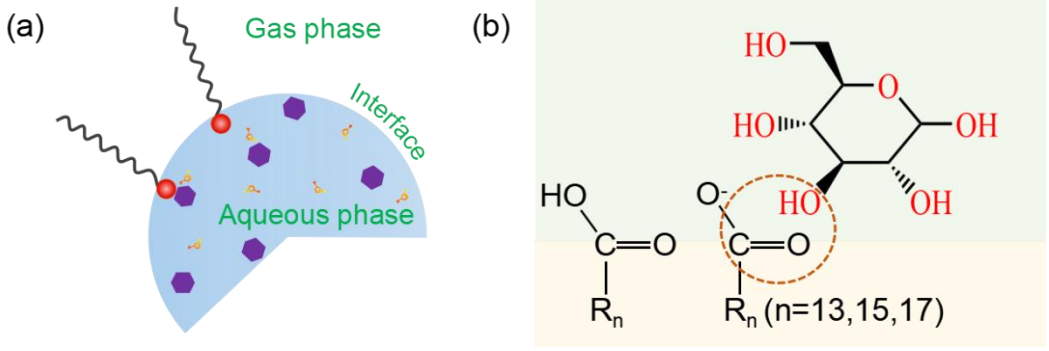

Figure 8. (a) Proposed model of fatty acid-saccharide interaction at the air/water interface. (b) Description of possible mechanisms of fatty acid-saccharide interaction at the air/water interface.

3.7 Atmospheric implications

Despite extensive efforts, the exhaustive relationships between ocean organic carbon pools and the chemical composition of SSAs are still outstanding. The coupling of this sea spray aerosol simulation generator with the interfacial monolayer model lays the foundation for further studies of the material relationship between the ocean and SSA. The research reported here yielded two key findings. First, the SSA production and particle size distribution are usually extremely sensitive to organic matter, and small saccharides dissolved in seawater are critical to the formation, size and composition of SSA. Our results strongly support those saccharides can greatly promote the generation of SSA particles and make SSA show core-shell morphology characteristics. A previous study revealed that the SSA number concentration in coastal samples was inversely correlated with salinity, with several organic tracers, including dissolved and chromophoric organic carbon (DOC, CDOM), marine microgels, and chlorophyll a (Chl-a) being positively correlated, but not associated with viral and bacterial abundances (Park et al., 2019). However, it is more complex in the real-world environment where the influencing factors are compounded. Other limitations to this study include the limited representation, by the simple chemical structural models, of the myriad complex biomolecules that exist in the ocean,

spanning dissolved, colloidal and particulate matter. It is recommended that future studies targeting the production and property of SSA include the effects of different types of organic matter to determine whether they fully mimic the arrays of SSA particles, and include more complete organic matter systems as well as biological species.

Second, it has been suggested that the abundant organic content in SSA plays a key role in determining the cloud condensation nucleation and ice nucleating activity (O'dowd et al., 2004). Therefore, climate models demand a predictive representation of SSA chemical composition to accurately simulate climate processes in the marine boundary layer (Burrows et al., 2016; Bertram et al., 2018). However, the source of organic enrichment observed in SSA remains speculative, which poses challenges to the modeling of the aerosol impact on atmospheric chemistry and climate science. A recent study has raised that the cooperative adsorption of saccharides with insoluble lipid monolayers may make important contributions to the sea spray aerosols and even have climatic consequences with broad research prospects (Burrows et al., 2014). Their team recently developed a process model for understanding the feedback relationship between marine biology, sea spray organic matter, and climate, called OCEANFILMS (Organic Compounds from Ecosystems to Aerosols: Natural Films and Interfaces via Langmuir Molecular Surfactants) sea spray organic aerosol emissions – implementation in a global climate model and impacts on clouds (Burrows et al., 2022). In this work, we used the Langmuir monolayer to model possible interactions between subphase soluble saccharides and surface fatty acid

molecules. A subsequent study used infrared reflection-absorption spectroscopy to determine the interaction mechanism between two simple soluble saccharides and tightly packed fatty acids monolayers at the air/water interface. Combining the above experimental results, we infer that the hydrogen bonding interaction between saccharides and the carbonyl group of surface insoluble fatty acid molecules contributes to its transfer from the ocean to the atmosphere. At present, this mechanism of saccharides transfer and enrichment has not been emphasized in the model describing SSA formation. Furthermore, our results may be an effective complement and development to OCEANFILMS model theory, and by adding the chemical interaction between soluble saccharides and an insoluble fatty acid surfactant monolayer, the consistency of modeled sea spray chemistry with observed marine aerosol chemistry may be improved. To further examine the feasibility of the hydrogen bonding mechanism as an interfacial organic enrichment mechanism, it is necessary to further explore and verify the interaction of other carbohydrates with common surface-insoluble molecules in future studies.

4 Conclusions

In summary, we simulated the production of SSA in natural seawater spiked with two common soluble saccharides using a plunging water jet generator and revealed the possible mechanism of saccharide transfer from bulk seawater into SSA combined with surface sensitive infrared spectroscopy techniques. We confirmed that glucose and trehalose can significantly promote the production of SSA and alter the surface

morphology of SSA particles. This highlights the potential for a direct oceanic source of carbohydrate organics through bubble bursting. In addition, trehalose showed stronger promoting ability than glucose, while the surface fatty acid layer played an inhibitory role. Using the mixture of saturated fatty acids MA, PA and SA as the proxy of SSA surface film, the π-A isotherms provided strong evidence that saccharides can interact with insoluble fatty acid monolayers and be adsorbed at the monolayer, which caused expansion of the monolayer and made the films heterogeneous. According to the IRRAS spectra, soluble saccharides did not produce a significant impact on the order of fatty acid alkyl chains. We further infer that soluble saccharides are mainly located on the subsurface below the monolayer, and interact with carbonyl groups of fatty acids by forming hydrogen bonds to facilitate their sea-air transfer. Crucially, this work provides physical and molecular signatures of potentially important saccharides transfer mechanism with general implications for understanding how saccharide-lipid interactions affect sea spray aerosol systems for real-world.

Data availability

Data are available by contacting the corresponding author.

Supplement

The supplement related to this article is available online at:

Author contributions

MX: conceived the experiment, data curation, formal analysis, writing original draft, writing-review & editing. NTT: writing - review & editing. JL: writing - review & editing. LD: supervision, conceived the experiment, funding acquisition, writing - review & editing.

Competing interests

The author declare that they have no conflict of interest.

Financial support

The authors acknowledge support from National Natural Science Foundation of China (22076099, 21876098), Youth Innovation Program of Universities in Shandong Province (2019KJD007), and Fundamental Research Fund of Shandong University (2020QNQT012).

References

Bertram, T. H., Cochran, R. E., Grassian, V. H., and Stone, E. A.: Sea spray aerosol chemical composition: Elemental and molecular mimics for laboratory studies of heterogeneous and multiphase reactions, Chem. Soc. Rev., 47, 2374-2400, 10.1039/c7cs00008a, 2018.

Blackshaw, K. J., Varmecky, M. G., and Patterson, J. D.: Interfacial structure and partitioning of nitrate ions in reverse micelles, J. Phys. Chem. A, 123, 336-342, 10.1021/acs.jpca.8b09751, 2019.

Brooks, S. D. and Thornton, D. C. O.: Marine aerosols and clouds, Annu. Rev. Mar. Sci., 10, 289-313, 10.1146/annurev-marine-121916-063148, 2018.

Burrows, S. M., Ogunro, O., Frossard, A. A., Russell, L. M., Rasch, P. J., and Elliott, S. M.: A physically based framework for modeling the organic fractionation of sea spray aerosol from bubble film Langmuir equilibria, Atmos. Chem. Phys., 14, 13601-13629, 10.5194/acp-14-13601-2014, 2014.

Burrows, S. M., Gobrogge, E., Fu, L., Link, K., Elliott, S. M., Wang, H. F., and Walker, R.: OCEANFILMS-2: Representing coadsorption of saccharides in marine films and potential impacts on modeled marine aerosol chemistry, Geophys. Res. Lett., 43, 8306-8313, 10.1002/2016gl069070, 2016.

Burrows, S. M., Easter, R. C., Liu, X. H., Ma, P. L., Wang, H. L., Elliott, S. M., Singh, B., Zhang, K., and Rasch, P. J.: OCEANFILMS (Organic Compounds from Ecosystems to Aerosols: Natural Films and Interfaces via Langmuir Molecular Surfactants) sea spray organic aerosol emissions - implementation in a global climate model and impacts on clouds, Atmos. Chem. Phys., 22, 5223-5251, 10.5194/acp-22-5223-2022, 2022.

Carter-Fenk, K. A. and Allen, H. C.: Collapse mechanisms of nascent and aged sea spray aerosol proxy films, Atmosphere, 9, 503, ARTN 503 10.3390/atmos9120503, 2018.

Christiansen, S., Salter, M. E., Gorokhova, E., Nguyen, Q. T., and Bilde, M.: Sea spray aerosol formation: Laboratory results on the role of air entrainment, water temperature and phytoplankton biomass, Environ. Sci. Technol., 53, 13107-13116, 10.1021/acs.est.9b04078, 2019.

Clark, G. A., Henderson, J. M., Heffern, C., Akgun, B., Majewski, J., and Lee, K. Y. C.: Synergistic interactions of sugars/polyols and monovalent salts with phospholipids depend upon sugar/polyol complexity and anion identity, Langmuir, 31, 12688-12698, 10.1021/acs.langmuir.5b02815, 2015.

Cochran, R. E., Laskina, O., Jayarathne, T., Laskin, A., Laskin, J., Lin, P., Sultana, C., Lee, C., Moore, K. A., Cappa, C. D., Bertram, T. H., Prather, K. A., Grassian, V. H., and Stone, E. A.: Analysis of organic anionic surfactants in fine and coarse fractions of freshly emitted sea spray aerosol, Environ. Sci. Technol., 50, 2477-2486, 10.1021/acs.est.5b04053, 2016.

Cochran, R. E., Laskina, O., Trueblood, J. V., Estillore, A. D., Morris, H. S., Jayarathne, T., Sultana, C. M., Lee, C., Lin, P., Laskin, J., Laskin, A., Dowling, J. A.,

Qin, Z., Cappa, C. D., Bertram, T. H., Tivanski, A. V., Stone, E. A., Prather, K. A., and Grassian, V. H.: Molecular diversity of sea spray aerosol particles: Impact of ocean biology on particle composition and hygroscopicity, Chem, 2, 655-667, 10.1016/j.chempr.2017.03.007, 2017.
Cravigan, L. T., Mallet, M. D., Vaattovaara, P., Harvey, M. J., Law, C. S., Modini, R. L., Russell, L. M., Stelcer, E., Cohen, D. D., Olsen, G., Safi, K., Burrell, T. J., and Ristovski, Z.: Sea spray aerosol organic enrichment, water uptake and surface tension effects, Atmos. Chem. Phys., 20, 7955-7977, 10.5194/acp-20-7955-2020, 2020.
Crowe, J. H., Whittam, M. A., Chapman, D., and Crowe, L. M.: Interactions of phospholipid monolayers with carbohydrates, Biochim Biophys Acta, 769, 151-159, 10.1016/0005-2736(84)90018-x, 1984.
Cunliffe, M., Engel, A., Frka, S., Gašparović, B., Guitart, C., Murrell, J. C., Salter, M., Stolle, C., Upstill-Goddard, R., and Wurl, O.: Sea surface microlayers: A unified physicochemical and biological perspective of the air–ocean interface, Prog. Oceanogr., 109, 104-116, 10.1016/j.pocean.2012.08.004, 2013.
de Vasquez, M. G. V., Rogers, M. M., Carter-Fenk, K. A., and Allen, H. C.: Discerning poly- and monosaccharide enrichment mechanisms: Alginate and glucuronate adsorption to a stearic acid sea surface microlayer, ACS Earth Space Chem., 6, 1581-1595, 10.1021/acsearthspacechem.2c00066, 2022.
Deane, G. B. and Stokes, M. D.: Scale dependence of bubble creation mechanisms in breaking waves, Nature, 418, 839-844, 10.1038/nature00967, 2002.
Elliott, S., Burrows, S. M., Deal, C., Liu, X., Long, M., Ogunro, O., Russell, L. M., and Wingenter, O.: Prospects for simulating macromolecular surfactant chemistry at the ocean-atmosphere boundary, Environ. Res. Lett., 9, 064012, 10.1088/1748-9326/9/6/064012, 2014.
Estillore, A. D., Morris, H. S., Or, V. W., Lee, H. D., Alves, M. R., Marciano, M. A., Laskina, O., Qin, Z., Tivanski, A. V., and Grassian, V. H.: Linking hygroscopicity and the surface microstructure of model inorganic salts, simple and complex carbohydrates, and authentic sea spray aerosol particles, Phys. Chem. Chem. Phys., 19, 21101-21111, 10.1039/c7cp04051b, 2017.
Facchini, M. C., Rinaldi, M., Decesari, S., Carbone, C., Finessi, E., Mircea, M., Fuzzi, S., Ceburnis, D., Flanagan, R., Nilsson, E. D., de Leeuw, G., Martino, M., Woeltjen, J., and O'Dowd, C. D.: Primary submicron marine aerosol dominated by insoluble organic colloids and aggregates, Geophys. Res. Lett., 35, L17814, 10.1029/2008gl034210, 2008.
Frossard, A. A., Russell, L. M., Burrows, S. M., Elliott, S. M., Bates, T. S., and Quinn, P. K.: Sources and composition of submicron organic mass in marine aerosol particles, J. Geophys. Res.-Atmos., 119, 12977-13003, 10.1002/2014jd021913, 2014.
Fuentes, E., Coe, H., Green, D., de Leeuw, G., and McFiggans, G.: Laboratory-generated primary marine aerosol via bubble-bursting and atomization, Atmos. Meas. Tech., 3, 141-162, 10.5194/amt-3-141-2010, 2010.
Gericke, A. and Huhnerfuss, H.: In-situ investigation of saturated long-chain fatty-acids at the air-water interface by external Infrared reflection-absorption spectrometry, J. Phys. Chem., 97, 12899-12908, 10.1021/j100151a044, 1993.

780 Hasenecz, E. S., Kaluarachchi, C. P., Lee, H. D., Tivanski, A. V., and Stone, E. A.:
781 Saccharide transfer to sea spray aerosol enhanced by surface activity, calcium, and
782 protein interactions, ACS Earth Space Chem., 3, 2539-2548,
783 10.1021/acsearthspacechem.9b00197, 2019.
784 Hasenecz, E. S., Jayarathne, T., Pendergraft, M. A., Santander, M. V., Mayer, K. J.,
785 Sauer, J., Lee, C., Gibson, W. S., Kruse, S. M., Malfatti, F., Prather, K. A., and Stone,
786 E. A.: Marine bacteria affect saccharide enrichment in sea spray aerosol during a
787 phytoplankton bloom, ACS Earth Space Chem., 4, 1638-1649,
788 10.1021/acsearthspacechem.0c00167, 2020.
789 Hawkins, L. N. and Russell, L.: Polysaccharides, proteins, and phytoplankton
790 fragments: Four chemically distinct types of marine primary organic aerosol classified
791 by single particle spectromicroscopy, Adv. Meteorol., 2010, 612132,
792 10.1155/2010/612132, 2010.
793 Hultin, K. A. H., Nilsson, E. D., Krejci, R., Martensson, E. M., Ehn, M., Hagstrom, A.,
794 and de Leeuw, G.: In situ laboratory sea spray production during the Marine Aerosol
795 Production 2006 cruise on the northeastern Atlantic Ocean, J. Geophys. Res.-Atmos.,
796 115, D06201, 10.1029/2009jd012522, 2010.
797 Johann, R., Vollhardt, D., and Mohwald, H.: Study of the pH dependence of head
798 group bonding in arachidic acid monolayers by polarization modulation infrared
799 reflection absorption spectroscopy, Colloid Surf. A-Physicochem. Eng. Asp., 182,
800 311-320, 10.1016/s0927-7757(00)00812-8, 2001.
801 Kapla, J., Engstrom, O., Stevensson, B., Wohlert, J., Widmalm, G., and Maliniak, A.:
802 Molecular dynamics simulations and NMR spectroscopy studies of trehalose-lipid
803 bilayer systems, Phys. Chem. Chem. Phys., 17, 22438-22447, 10.1039/c5cp02472b,
804 2015.
805 King, S. M., Butcher, A. C., Rosenoern, T., Coz, E., Lieke, K. I., de Leeuw, G.,
806 Nilsson, E. D., and Bilde, M.: Investigating primary marine aerosol properties: CCN
807 activity of sea salt and mixed inorganic-organic particles, Environ. Sci. Technol., 46,
808 10405-10412, 10.1021/es300574u, 2012.
809 Lambruschini, C., Relini, A., Ridi, A., Cordone, L., and Gliozzi, A.: Trehalose
810 interacts with phospholipid polar heads in Langmuir monolayers, Langmuir, 16,
811 5467-5470, 10.1021/la991641e, 2000.
812 Lee, C., Dommer, A. C., Schiffer, J. M., Amaro, R. E., Grassian, V. H., and Prather, K.
813 A.: Cation-driven lipopolysaccharide morphological changes impact heterogeneous
814 reactions of nitric acid with sea spray aerosol particles, J. Phys. Chem. Lett., 12,
815 5023-5029, 10.1021/acs.jpclett.1c00810, 2021.
816 Lee, H. D., Wigley, S., Lee, C., Or, V. W., Hasenecz, E. S., Stone, E. A., Grassian, V.
817 H., Prather, K. A., and Tivanski, A. V.: Physicochemical mixing state of sea spray
818 aerosols: Morphologies exhibit size dependence, ACS Earth Space Chem., 4,
819 1604-1611, 10.1021/acsearthspacechem.0c00153, 2020.
820 Lee, K. Y. C.: Collapse mechanisms of Langmuir monolayers, Annu. Rev. Phys.
821 Chem., 59, 771-791, 10.1146/annurev.physchem.58.032806.104619, 2008.
822 Li, S. Y., Jiang, X. T., Roveretto, M., George, C., Liu, L., Jiang, W., Zhang, Q. Z.,
823 Wang, W. X., Ge, M. F., and Du, L.: Photochemical aging of atmospherically reactive

organic compounds involving brown carbon at the air-aqueous interface, Atmos. Chem. Phys., 19, 9887-9902, 10.5194/acp-19-9887-2019, 2019.
Link, K. A., Spurzem, G. N., Tuladhar, A., Chase, Z., Wang, Z. M., Wang, H. F., and Walker, R. A.: Cooperative adsorption of trehalose to DPPC monolayers at the water-air interface studied with vibrational sum frequency generation, J. Phys. Chem. B, 123, 8931-8938, 10.1021/acs.jpcb.9b07770, 2019a.
Link, K. A., Spurzem, G. N., Tuladhar, A., Chase, Z., Wang, Z. M., Wang, H. F., and Walker, R. A.: Organic enrichment at aqueous interfaces: Cooperative adsorption of glucuronic acid to DPPC monolayers studied with vibrational sum frequency generation, J. Phys. Chem. A, 123, 5621-5632, 10.1021/acs.jpca.9b02255, 2019b.
Liu, L. R., Du, L., Xu, L., Li, J. L., and Tsona, N. T.: Molecular size of surfactants affects their degree of enrichment in the sea spray aerosol formation, Environ. Res., 206, 112555, 10.1016/j.envres.2021.112555, 2022.
Luzardo, M. D., Amalfa, F., Nunez, A. M., Diaz, S., de Lopez, A. C. B., and Disalvo, E. A.: Effect of trehalose and sucrose on the hydration and dipole potential of lipid bilayers, Biophys. J., 78, 2452-2458, 10.1016/s0006-3495(00)76789-0, 2000.
Lv, C., Tsona, N. T., and Du, L.: Sea spray aerosol formation: Results on the role of different parameters and organic concentrations from bubble bursting experiments, Chemosphere, 252, 126456, 10.1016/j.chemosphere.2020.126456, 2020.
Modini, R. L., Russell, L. M., Deane, G. B., and Stokes, M. D.: Effect of soluble surfactant on bubble persistence and bubble-produced aerosol particles, J. Geophys. Res.-Atmos., 118, 1388-1400, 10.1002/jgrd.50186, 2013.
Muro, M., Itoh, Y., and Hasegawa, T.: A conformation and orientation model of the carboxylic group of fatty acids dependent on chain length in a Langmuir monolayer film studied by polarization-modulation infrared reflection absorption spectroscopy, J. Phys. Chem. B, 114, 11496-11501, 10.1021/jp105862q, 2010.
O'Dowd, C. D., Facchini, M. C., Cavalli, F., Ceburnis, D., Mircea, M., Decesari, S., Fuzzi, S., Yoon, Y. J., and Putaud, J. P.: Biogenically driven organic contribution to marine aerosol, Nature, 431, 676-680, 10.1038/nature02959, 2004.
Pakulski, J. D. and Benner, R.: An improved method for the hydrolysis and MBTH analysis of dissolved and particulate carbohydrates in seawater, Mar. Chem., 40, 143-160, 10.1016/0304-4203(92)90020-B, 1992.
Park, J., Dall'Osto, M., Park, K., Kim, J. H., Park, J., Park, K. T., Hwang, C. Y., Jang, G. I., Gim, Y., Kang, S., Park, S., Jin, Y. K., Yum, S. S., Simo, R., and Yoon, Y. J.: Arctic primary aerosol production strongly influenced by riverine organic matter, Environ. Sci. Technol., 53, 8621-8630, 10.1021/acs.est.9b03399, 2019.
Partanen, A. I., Dunne, E. M., Bergman, T., Laakso, A., Kokkola, H., Ovadnevaite, J., Sogacheva, L., Baisnee, D., Sciare, J., Manders, A., O'Dowd, C., de Leeuw, G., and Korhonen, H.: Global modelling of direct and indirect effects of sea spray aerosol using a source function encapsulating wave state, Atmos. Chem. Phys., 14, 11731-11752, 10.5194/acp-14-11731-2014, 2014.
Pavinatto, F. J., Caseli, L., Pavinatto, A., dos Santos, D. S., Nobre, T. M., Zaniquelli, M. E. D., Silva, H. S., Miranda, P. B., and de Oliveira, O. N.: Probing chitosan and phospholipid interactions using Langmuir and Langmuir-Blodgett films as cell

membrane models, Langmuir, 23, 7666-7671, 10.1021/la700856a, 2007.
Perkins, R. and Vaida, V.: Phenylalanine increases membrane permeability, J. Am. Chem. Soc., 139, 14388-14391, 10.1021/jacs.7b09219, 2017.
Prather, K. A., Bertram, T. H., Grassian, V. H., Deane, G. B., Stokes, M. D., DeMott, P. J., Aluwihare, L. I., Palenik, B. P., Azam, F., Seinfeld, J. H., Moffet, R. C., Molina, M. J., Cappa, C. D., Geiger, F. M., Roberts, G. C., Russell, L. M., Ault, A. P., Baltrusaitis, J., Collins, D. B., Corrigan, C. E., Cuadra-Rodriguez, L. A., Ebben, C. J., Forestieri, S. D., Guasco, T. L., Hersey, S. P., Kim, M. J., Lambert, W. F., Modini, R. L., Mui, W., Pedler, B. E., Ruppel, M. J., Ryder, O. S., Schoepp, N. G., Sullivan, R. C., and Zhao, D. F.: Bringing the ocean into the laboratory to probe the chemical complexity of sea spray aerosol, Proc. Natl. Acad. Sci. U. S. A., 110, 7550-7555, 10.1073/pnas.1300262110, 2013.
Quinn, P. K., Coffman, D. J., Johnson, J. E., Upchurch, L. M., and Bates, T. S.: Small fraction of marine cloud condensation nuclei made up of sea spray aerosol, Nat. Geosci., 10, 674-679, 10.1038/ngeo3003, 2017.
Quinn, P. K., Collins, D. B., Grassian, V. H., Prather, K. A., and Bates, T. S.: Chemistry and related properties of freshly emitted sea spray aerosol, Chem. Rev., 115, 4383-4399, 10.1021/cr500713g, 2015.
Quinn, P. K., Bates, T. S., Schulz, K. S., Coffman, D. J., Frossard, A. A., Russell, L. M., Keene, W. C., and Kieber, D. J.: Contribution of sea surface carbon pool to organic matter enrichment in sea spray aerosol, Nat. Geosci., 7, 228-232, 10.1038/ngeo2092, 2014.
Ray, K. K., Lee, H. D., Gutierrez, M. A., Chang, F. J., and Tivanski, A. V.: Correlating 3D morphology, phase state, and viscoelastic properties of individual substrate-deposited particles, Anal. Chem., 91, 7621-7630, 10.1021/acs.analchem.9b00333, 2019.
Ruehl, C. R., Davies, J. F., and Wilson, K. R.: An interfacial mechanism for cloud droplet formation on organic aerosols, Science, 351, 1447-1450, 10.1126/science.aad4889, 2016.
Russell, L. M., Hawkins, L. N., Frossard, A. A., Quinn, P. K., and Bates, T. S.: Carbohydrate-like composition of submicron atmospheric particles and their production from ocean bubble bursting, Proc. Natl. Acad. Sci. U. S. A., 107, 6652-6657, 10.1073/pnas.0908905107, 2010.
Schill, S., Burrows, S., Hasenecz, E., Stone, E., and Bertram, T.: The impact of divalent cations on the enrichment of soluble saccharides in primary sea spray aerosol, Atmosphere, 9, 476, 10.3390/atmos9120476, 2018.
Schmitt-Kopplin, P., Liger-Belair, G., Koch, B. P., Flerus, R., Kattner, G., Harir, M., Kanawati, B., Lucio, M., Tziotis, D., Hertkorn, N., and Gebefugi, I.: Dissolved organic matter in sea spray: a transfer study from marine surface water to aerosols, Biogeosciences, 9, 1571-1582, 10.5194/bg-9-1571-2012, 2012.
Unger, I., Saak, C. M., Salter, M., Zieger, P., Patanen, M., and Bjorneholm, O.: Influence of organic acids on the surface composition of sea spray aerosol, J. Phys. Chem. A, 124, 422-429, 10.1021/acs.jpca.9b09710, 2020.
van Pinxteren, M., Muller, C., Iinuma, Y., Stolle, C., and Herrmann, H.: Chemical

characterization of dissolved organic compounds from coastal sea surface micro layers (Baltic Sea, Germany), Environ. Sci. Technol., 46, 10455-10462, 10.1021/es204492b, 2012.
van Pinxteren, M., Fomba, K. W., Triesch, N., Stolle, C., Wurl, O., Bahlmann, E., Gong, X. D., Voigtlander, J., Wex, H., Robinson, T. B., Barthel, S., Zeppenfeld, S., Hoffmann, E. H., Roveretto, M., Li, C. L., Grosselin, B., Daele, V., Senf, F., van Pinxteren, D., Manzi, M., Zabalegui, N., Frka, S., Gasparovic, B., Pereira, R., Li, T., Wen, L., Li, J. R., Zhu, C., Chen, H., Chen, J. M., Fiedler, B., Von Tumpling, W., Read, K. A., Punjabi, S., Lewis, A. C., Hopkins, J. R., Carpenter, L. J., Peeken, I., Rixen, T., Schulz-Bull, D., Monge, M. E., Mellouki, A., George, C., Stratmann, F., and Herrmann, H.: Marine organic matter in the remote environment of the Cape Verde islands - an introduction and overview to the MarParCloud campaign, Atmos. Chem. Phys., 20, 6921-6951, 10.5194/acp-20-6921-2020, 2020.
Villarreal, M. A., Diaz, S. B., Disalvo, E. A., and Montich, G. G.: Molecular dynamics simulation study of the interaction of trehalose with lipid membranes, Langmuir, 20, 7844-7851, 10.1021/la0494851, 2004.
Wang, X. F., Deane, G. B., Moore, K. A., Ryder, O. S., Stokes, M. D., Beall, C. M., Collins, D. B., Santander, M. V., Burrows, S. M., Sultana, C. M., and Prather, K. A.: The role of jet and film drops in controlling the mixing state of submicron sea spray aerosol particles, Proc. Natl. Acad. Sci. U. S. A., 114, 6978-6983, 10.1073/pnas.1702420114, 2017.
Wurl, O., Ekau, W., Landing, W. M., and Zappa, C. J.: Sea surface microlayer in a changing ocean - A perspective, Elementa. Sci. Anthrop., 5, 31, 10.1525/elementa.228, 2017.
Xu, M. L., Tsona, N. T., Cheng, S. M., Li, J. L., and Du, L.: Unraveling interfacial properties of organic-coated marine aerosol with lipase incorporation, Sci. Total Environ., 782, 146893, 10.1016/j.scitotenv.2021.146893, 2021.
Xu, W., Ovadnevaite, J., Fossum, K. N., Lin, C. S., Huang, R. J., Ceburnis, D., and O'Dowd, C.: Sea spray as an obscured source for marine cloud nuclei, Nat. Geosci., 15, 282-286, 10.1038/s41561-022-00917-2, 2022.
You, X., Lee, E., Xu, C., and Baiz, C. R.: Molecular mechanism of cell membrane protection by sugars: A study of interfacial H-Bond networks, J. Phys. Chem. Lett., 12, 9602-9607, 10.1021/acs.jpclett.1c02451, 2021.
Zeppenfeld, S., van Pinxteren, M., van Pinxteren, D., Wex, H., Berdalet, E., Vaque, D., Dall'Osto, M., and Herrmann, H.: Aerosol marine primary carbohydrates and atmospheric transformation in the Western Antarctic Peninsula, ACS Earth Space Chem., 5, 1032-1047, 10.1021/acsearthspacechem.0c00351, 2021.